J. Plant Biol. (2016) 59:358-368
DOI 10.1007/s12374-016-0056-x

ORIGINAL ARTICLE

Gibberellin and Auxin Signals Control Scape Cell Elongation and Proliferation in *Agapanthus praecox* ssp. *orientalis*

Jian-hua Yue, Di Zhang, Li Ren and Xiao-hui Shen*

Key Laboratory of Urban Agriculture (South) Ministry of Agriculture, School of Agriculture and Biology, Shanghai Jiao Tong University, Shanghai 200240, PR China

Received: Jan 30, 2016 / Accepted: April 15, 2016

Abstract Plant height is determined by the processes of cell proliferation and elongation. Plant hormones play key roles in a species-dependent manner in these processes. We used paclobutrazol (PAC) at 400 $mg \cdot L^{-1}$ in this study to spray *Agapanthus praecox* ssp. *orientalis* plants in order to induce dwarf scape (inflorescence stem). Morphological examination showed that PAC reduced scape height by inhibiting the cell elongation by 54.56% and reducing cell proliferation by 10.45% compared to the control. Quantification and immunolocalization of endogenous gibberellins (GAs) and indole-3-acetic acid (IAA) showed that the GA_1, GA_3, and GA_4 levels and the IAA gradient were reduced. Among these hormones, GA_4 was the key component of GAs, which decreased 59.51-92.01% compared to the control in scape. The expression of cell wall synthesis related genes cellulose synthase (*CESA*) and UDP-glucuronic acid decarboxylase (*UXS*) were upregulated significantly, whereas cell wall loosening gene xyloglucan endotransglucosylase 2 (*XET2*) was downregulated by 99.99% surprisingly. Correlation analysis suggested GA regulated cell elongation and auxin modulated cell proliferation in *Agapanthus* scape. Additionally, the accumulation of sugars played roles in cell wall synthesis and cell expansion. These results indicated GA and IAA signals triggered a downstream signaling cascade, controlled cell expansion and proliferation during scape elongation.

Keywords: *Agapanthus praecox* ssp. *orientalis*, Cell expansion, Cell proliferation, Dwarf, Gibberellin, Paclobutrazol

Introduction

Agapanthus praecox ssp. *orientalis* is a monocotyledonous perennial bulbous plant. It is a popular potted plant, cut flower, and landscape plant, and is characterized by a tuberous rootstock, large number of flowers and straight, tall, thick scape (inflorescence stem) (Zhang et al. 2013). In *Agapanthus*, the initial flowering takes 3-4 years, and this species then flowers annually thereafter. In optimum conditions, the height of *Agapanthus* scape can reach about 1 m within 2 months during flowering. In bulbous-flower, scape height is considered as an important phenotype affecting its ornamental value. *Agapanthus*, due to its fast growth in inflorescence stem, is suggested to be an ideal plant for the scape development study.

Plant hormones play important roles in the regulation of plant development (Davière and Achard 2016). In one of our previous studies, we analyzed the contents of gibberellins (GAs), indole-3-acetic acid (IAA), cytokinins (CKs) and abscisic acids (ABAs) during flowering time of *A. praecox* ssp. *orientalis*; the results showed that GAs and IAA played important roles in flowering and scape development, whereas starch and sucrose metabolism provide nutrients to this process. Furthermore, we used plant growth regulators in flowering, and the results showed that paclobutrazol (PAC, an inhibitor of GA biosynthesis) inhibited scape elongation significantly (Fig. S1), suggesting that GAs played crucial roles in *Agapanthus* scape height control (Zhang et al. 2014).

Plant hormones are involved in the program of cell proliferation and expansion, which determine the final plant height (Hepworth and Lenhard 2014). In *Zea mays*, the *d2003* mutant has shortened internodes because of the reduced cell numbers, not the cell elongation (Lv, Zheng et al. 2014), whereas in *Triticum aestivum*, *Rht23* reduced plant height by controlling cell expansion (Chen et al. 2015). In *Arabidopsis thaliana*, *cdkf;1-1* mutants are defective in both cell division and cell expansion (Takatsuka et al. 2009). Furthermore, hormonal signals coordinate regulated plant cell division and elongation organ-dependently and species-

*Corresponding author; Xiao-hui Shen
Tel : +86-21-34205736
E-mail : shenxh62@sjtu.edu.cn

dependently. For instance, *A. thaliana* GA 20-oxidase (*GA20ox*; EC 1.14.11.12) promotes both cell division and cell expansion in leaves, whereas *AtGA20ox* leads to cell internodes expansion and stimulates leave cell proliferation in *Z. mays* (Claeys et al. 2014). Similar patterns can be obtained in auxin, for IAA promotes cell division in tomato and cell expansion in *A. thaliana* (Vivian-Smith and Koltunow 1999; Serrani et al. 2007). Interestingly, IAA is also proved playing roles in plant height regulation, and some auxin-deficient dwarf plants show reduced apical dominance (Dai et al. 2006). Thus, the process of plant height development regulated by plant hormones is extremely complex.

Within plant hormones, GA is the major hormone that induces stem elongation in model plants, such as *A. thaliana*, *Nicotiana tabacum*, and *Oryza sativa* (Dayan et al. 2012; Topp and Rasmussen 2012; Ayano et al. 2014). Some mutants with lower GA levels present a dwarf phenotype. PAC inhibits the activity of *ent*-kaurene oxidase (*KO*) and disrupts GAs biosynthesis pathway; and plants always present a GA-deficient phenotype with PAC treatment because of lower GA levels (Christiaens et al. 2015). Besides, PAC affects GA signaling for the accumulation of DELLA proteins (such as GAI and RGA) (Feng, Martinez et al. 2008). The pathway of GAs syntheses is documented previously (Yamaguchi 2008; Topp and Rasmussen 2012). Several kinds of synthases are involved in the biosynthetic pathway of GAs, and among of these synthases, *GA20ox* is a crucial enzyme for the control of bioactive GAs, such as GA_1, GA_3 and GA_4 (Yamaguchi 2008). In the GA signaling pathway, GA binds to its receptor GIBBERELLIN INSENSITIVE DWARF1 (GID1), and forms complexes with DELLAs (Sun 2011). Then the complex formation usually leads to degradation of DELLAs by the ubiquitin-proteasome pathway (Topp and Rasmussen 2012). Although DELLAs are proved and regarded response for GA, some reports show that DELLAs regulate signaling of auxin (Nemhauser et al. 2006). IAA is synthesized by several pathways and transported by a polar manner. In the auxin signaling pathway, auxin/indole-3-acetic acid (*AUX/IAA*), small auxin up RNA (*SAUR*), and *GH3* were specifically induced by auxin and involved in the regulation of auxin signal transduction (Mashiguchi et al. 2011).

Plant hormones regulate stem elongation by regulating cell division and subsequent cell elongation, which requires a change in cell wall structure or synthesis of new cell wall (Chen et al. 2013). Cell wall modification determined the final size of plant cells. Cellulose and hemicelluloses are two of the main components of cell wall, which can be catalyzed by cellulose synthase (*CESA*; EC: 2.4.1.12) and UDP-glucuronic acid decarboxylase (*UXS*; EC: 4.1.1.35) respectively. Hemicelluloses are responsible for crosslinks between cellulose fibers. Xyloglucan endotransglucosylase (*XET*; EC: 2.4.1.207) contributes to cell wall loosening that allows cell enlargement, and GA induces the expression of *XET* (Cosgrove 2005; Zhu et al. 2012).

The disciplines of plant hormones regulating plant stem elongation have some commonality and some differences as well. In previous studies, many reports focused on hormone biosynthesis rather than the morphological and physiological investigation. This study aims to elucidate the comprehensive regulatory mechanisms of *Agapanthus* scape elongation. We used cell morphological observation and plant hormone quantification to identify the roles of GAs and IAA in cell proliferation and elongation; we combined cell size, cell wall components and cellular transcript data to elucidate the mechanisms of scape cell wall structure modification. This study provides information shedding new light into the mechanisms how scape development in bulbous plants is regulated.

Results

Quantification of Bioactive GAs and IAA

Endogenous, bioactive GAs quantification showed the contents of GAs decreased significantly with PAC treatment (Fig. 1A). In control scape, the concentrations of GA_1 and GA_3 were maintained at 0.04-0.18 $ng \cdot g^{-1} \cdot FW^{-1}$, however, GA_4

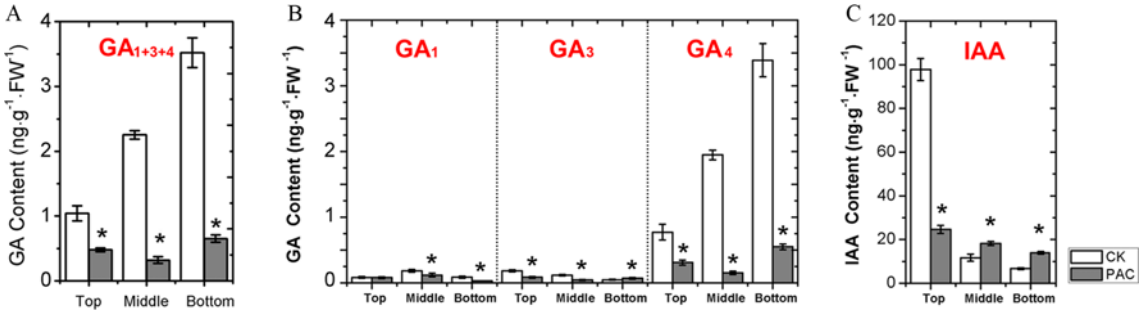

Fig. 1. Quantitative analyses of bioactive GAs and IAA in control and PAC-treated scape. Endogenous bioactive GAs levels (A, B) and IAA levels (C) in control and PAC-treated scape; data are means ± SD (n = 3). CK represents a control plant; PAC represents a PAC-treated plant. Asterisks indicate a significant difference ($P < 0.05$) compared with control.

accumulated at high concentrations of 0.77-3.39 $ng \cdot g^{-1} \cdot FW^{-1}$ (Fig. 1B), and increased continuously from top to bottom. After PAC treatment, the concentration of GA_4 decreased dramatically by 59.51-92.01% in scape (Fig. 1B). Similarly, the contents of GA_1 and GA_3 also decreased in the treated scape (Fig. 1B). In control plants, IAA concentrations decreased continuously from the top to bottom; with PAC treatment, IAA concentrations decreased 74.83% at the top, but increased 56.29% and 107.29% in the middle and bottom of the scape, respectively (Fig. 1C).

Immunolocalization of GAs and IAA

Immunolocalization of endogenous hormones showed that GAs and IAA were mainly localized in the cortex, cambium, and vascular bundles. Blank and negative controls showed no hormonal signals, indicating the lack of nonspecific immune signals in the scape tissues. The GAs and IAA signals accumulated in the cortex and cambium, suggesting that GAs and IAA possibly act as regulators for cambial development (Fig. 2A). Additionally, GAs and IAA signals were accumulated in the vascular bundles, indicating that these hormones were possibly transported in scape and PAC treatment triggered changes of hormones localization (Fig. 2B). GAs immunolocalization was accorded with GAs quantification; the GA signals accumulated at the bottom were stronger than at the top in control samples, and GAs immune signal was reduced in the PAC-treated samples (Fig. 2B). In contrast to GAs, the IAA signal at the top was stronger than at the bottom part, and IAA signal was reduced at the top and middle but increased in the bottom part of scape (Fig. 2B).

Expression Levels of GA and IAA Related Genes

GA biosynthesis- and signal-related genes were upregulated with PAC treatment. The expression levels of *GA20ox* were significantly upregulated 6.06, 37.34 and 16.21-fold change (FC) from top to bottom in scape, respectively (Fig. 3A).

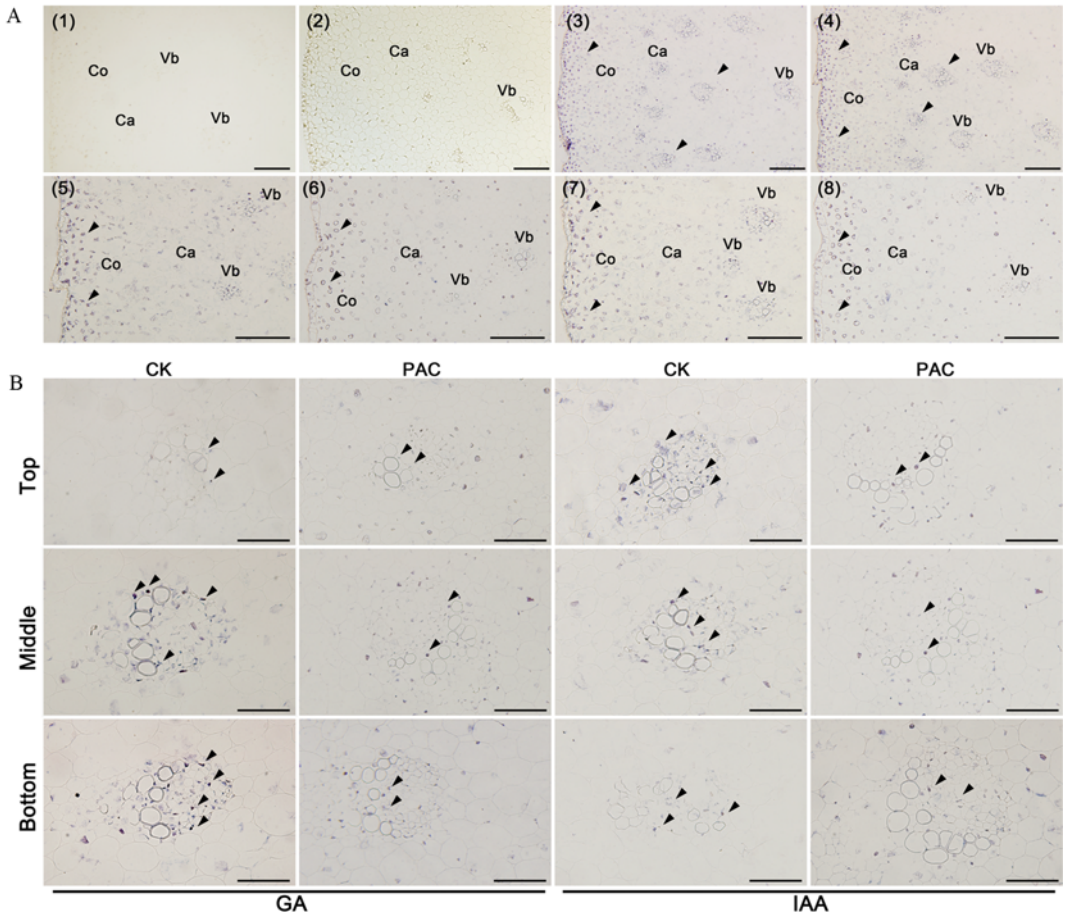

Fig. 2. Immunolocalization of GAs and IAA in scape of *A. praecox* ssp. *orientalis*. (A) Immunolocalization of GAs and IAA in cortex and cambium. bar = 100 μm. 1, blank control; 2, negative control; 3, immunolocalization of GAs; 4, Immunolocalization of IAA; 5, GAs localization in the cortex and cambium of control scape; 6, GAs localization in the cortex and cambium of PAC-treated scape; 7, IAA localization in the cortex and cambium of control scape; 8, IAA localization in the cortex and cambium of PAC-treated scape; Co, cortex; Ca, cambium; Vb, vascular bundle. (B) Immunolocalization of GAs and IAA in vascular bundle. bar = 50 μm. Top, middle, and bottom indicate immunolocalization in scape cross-sections in the top, middle, and bottom regions of the scape, respectively.

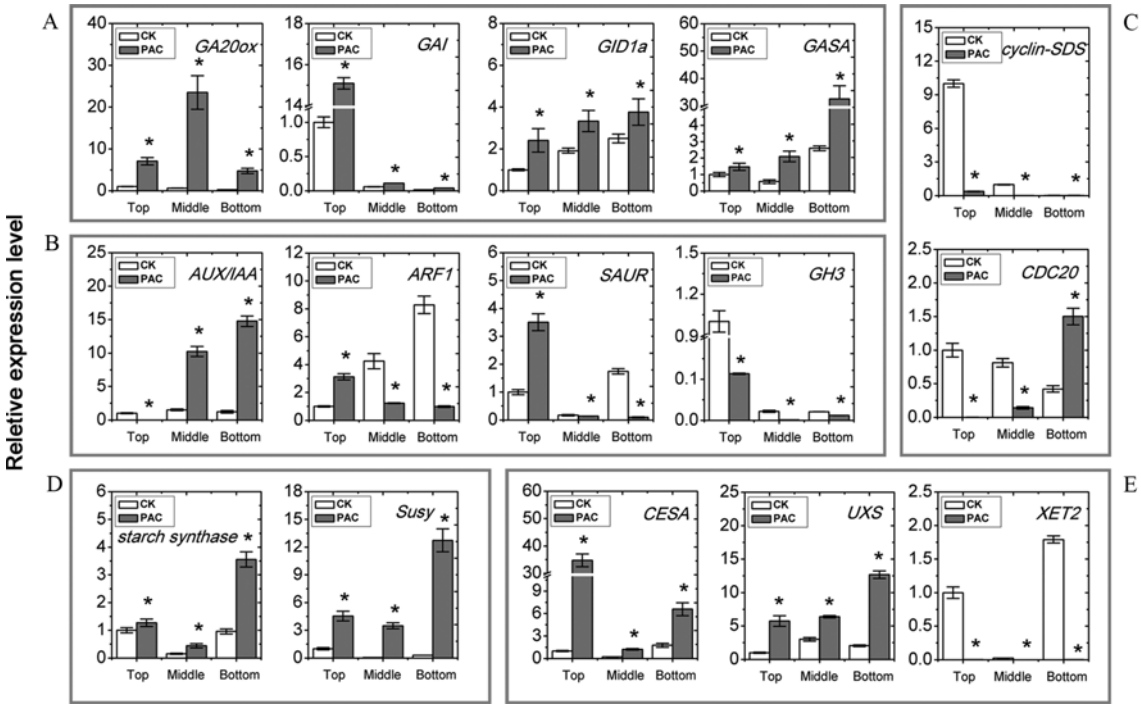

Fig. 3. Quantitative analyses of differentially expressed genes in control and PAC-treated scape. (A) GA-related genes. (B) Auxin-related genes. (C) Cell circle-related genes. (D) Starch and sucrose metabolism-related genes. (E) Cell wall modification-related genes. Data are means ± SD (n = 3). CK represents a control plant; PAC represents a PAC-treated plant. Asterisks indicate a significant difference (P < 0.05) compared with control.

Similar trends were observed in the expression levels of *GAI*, which increased 14.09, 0.85 and 1.61 (FC) at the top, middle, and bottom regions (Fig. 3A). Likewise, the GA receptor *GID1a* and GA-stimulated in Arabidopsis (*GASA*) were upregulated significantly (Fig. 3A). The above data indicated GA-related genes were upregulated with PAC treatment.

The expression of auxin signaling-related genes suggested IAA signal was also depressed in PAC-treated scape. *AUX/IAA* expression levels decreased significantly at the top part of the scape and increased in the middle and bottom parts of the scape (Fig. 3B). In contrast, the auxin response factor 1 (*ARF1*) and *SAUR* increased at the top, and decreased in the middle and bottom of the scape compared with controls, and the variation trend was accorded with IAA levels (Fig. 3B). Additionally, *GH3* was downregulated at each part of the scape (Fig. 3B). The expression patterns of these genes suggested that auxin signal was inhibited.

Plant Morphological Observation

PAC treatment led to obvious dwarf scape in *A. praecox* ssp. *orientalis* (Fig. 4). In control scape, the length reached 91.23 cm (Fig. 4B, C). However, the final length was significantly reduced by 54.56% in PAC-treated scape (Fig. 4D). Cell morphology showed the longitudinal lengths of cells were reduced significantly by 50.91% compared with control (Fig. 4G), indicated cell expansion was inhibited in response to GAs deficiency. The cell lengths were about 170-185 μm in control plants, whereas cell longitudinal size reduced 47.97-51.10% in dwarf scape (Fig. 4E, F). However, cell width showed no difference between control and dwarf samples (Fig. 4H). Additionally, cell number in the longitudinal direction decreased 10.45% compared with control (Fig. 4I). The above results indicated the dwarf scape reduced both cell proliferation and elongation. Furthermore, expression levels of cell cycle-related genes showed cell cycle was reduced. The expression of *cyclin-SDS* was downregulated by 96.24%, 98.56% and 13.13% in the apical, middle and basal parts in dwarf scape (Fig. 3C); meanwhile, the expression levels of cell division cycle 20 (*CDC20*) were decreased 99.93%, 82.66% at top, middle and increased 256.31% at bottom of the dwarf scape (Fig. 3C), suggesting the cell cycle was depressed in the dwarf scape.

Analysis of Sugars Accumulation and Cell Wall Modification

The increase of sugars accumulation was detected in dwarf scape suggested sugars metabolism possibly play roles in scape elongation. PAS staining showed the massive starch grains were accumulated in cambium cells and the vascular bundle in the PAC-treated scape (Fig. 5A). Consistent results

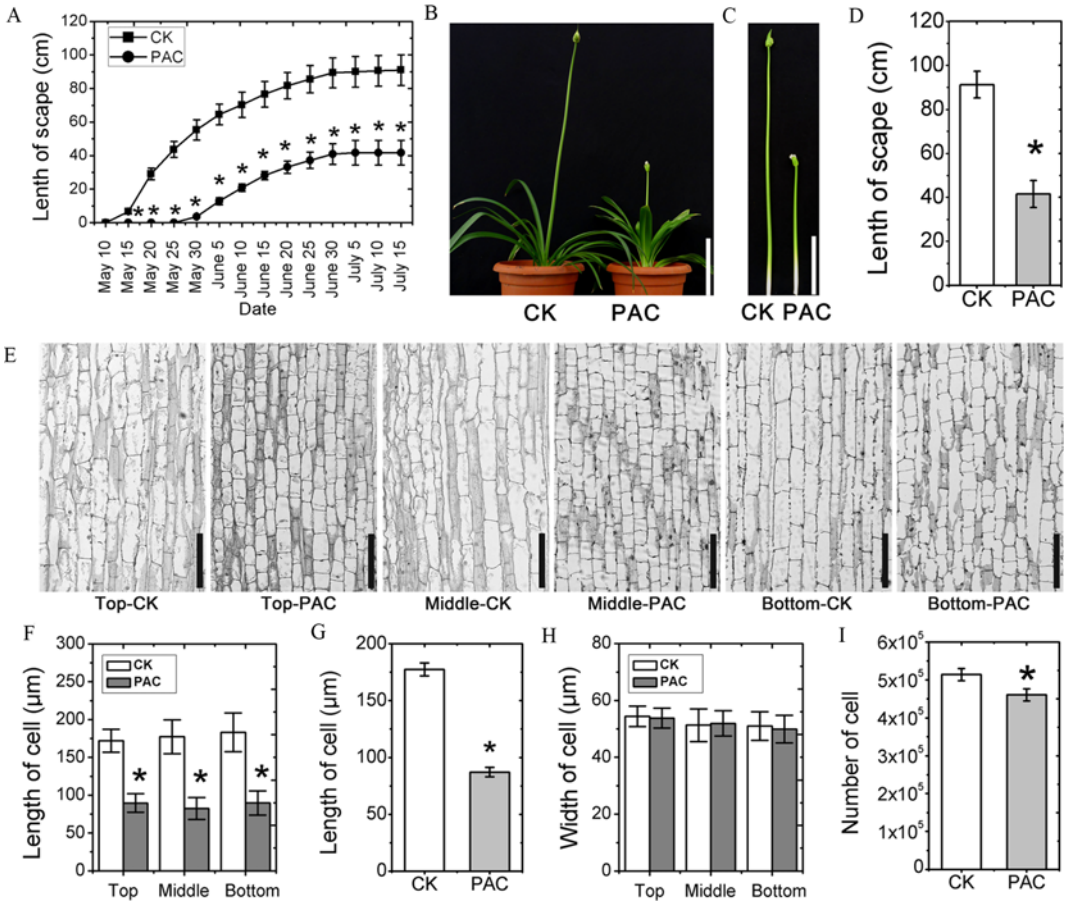

Fig. 4. Morphological analyses of control and PAC-treated scape of *A. praecox* ssp. *orientalis*. (A) PAC treatment induces dwarf scape in elongation stage; data are means ± SD (n = 3). (B) Morphological differences between control and PAC-treated plants; bar = 20 cm. (C) Scape of control and PAC-treated plants; bar = 20 cm. (D) Scape length; values are means ± SD (n = 3). (E) Longitudinal sections of scape observed by light microscopy; bar = 200 μm. (F) Cell length in top, middle and bottom; values are means ± SD (n = 10). (G) An average cell size; values are means ± SD (n = 3). (H) Cell width in top, middle and bottom; values are means ± SD (n = 10). (I) Cell number difference; data are means ± SD (n = 3). CK represents a control plant; PAC represents a PAC-treated plant. Asterisks indicate a significant difference ($P < 0.05$) compared with control.

were gained with starch quantification; after PAC treatment, the contents of starch increased 32.5-37.8% (Fig. 5B) and the contents of sucrose also increased 62.37-102.51% in dwarf scape (Fig. 5C). Furthermore, the expression levels of *starch synthase* (EC: 2.4.1.21) were upregulated 0.26-2.71 (FC) and sucrose synthase (*Susy*; EC: 2.4.1.13) were upregulated 3.54-85.05 (FC) in PAC-treated scape (Fig. 3D). The data above showed that dwarf scape with high levels of sugars accumulation.

The contents of cellulose and hemicelluloses in dwarf scape indicated that cell wall components changed obviously. The contents of cellulose were increased from 13.99%-16.36% in control scape to 22.25-25.58% in PAC-treated samples (Fig. 5D); and contents of hemicelluloses also increased from 10.23-11.64% in control scape to 13.96-16.54% in PAC-treated scape (Fig. 5E). The transcript levels of *CESA* and *UXS* were upregulated significantly in dwarf scape (Fig. 3E), which were accorded with the contents of cellulose and hemicelluloses. Notably, the expression of *XET2*, which cleaves xyloglucan hemicelluloses chain crosslink cellulose microfibrils, was decreased 99.99% in dwarf scape (Fig. 3E). The increased cellulose and hemicelluloses accumulation possibly contributed to cell size modification.

Correlation Analysis

Correlation analysis indicated GA promoted cell expansion and IAA regulated cell circle during *Agapanthus* scape development. Content of GA_{1+3+4} was positively correlated with the cell longitudinal length (Pearson correlation coefficient is 0.822, $P < 0.05$, Table 1), suggested bioactive GAs regulated scape cell length. Furthermore, the expression level of *XET2* was positively correlated with the level of

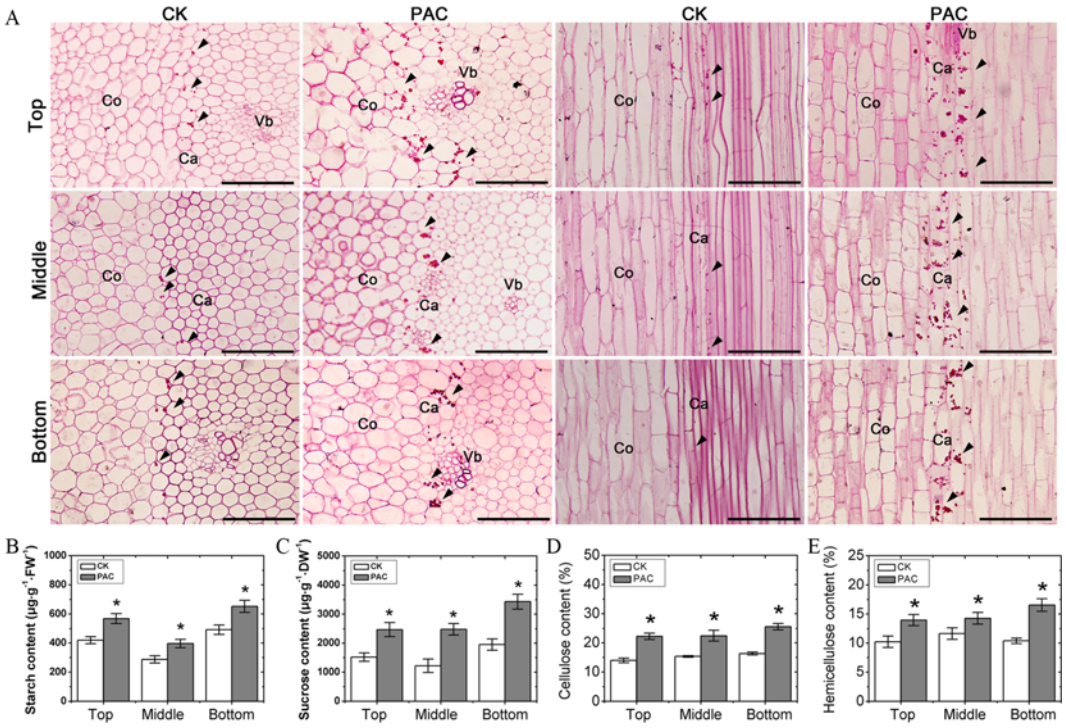

Fig. 5. Analyses of sugar accumulation and cell wall components in scape. (A) PAS staining of polysaccharide; starch grains are present in both cross-sections (left) and longitudinal-sections (right) of a control scape and PAC-treated scape; bar = 100 μm; Co, cortex; Ca, cambium; Vb, vascular bundle. (B) Starch content. (C) Sucrose content. (D) Cellulose content. (E) Hemicelluloses content. Data are means ± SD (n = 3). CK represents a control plant; PAC represents a PAC-treated plant. Asterisks indicate a significant difference (P < 0.05) compared with control.

Table 1. Correlation analysis of cell length, cell wall components, sugars and hormonal contents

	Cell length	Cellulose	Hemicelluloses	Starch	Sucrose	GA_1	GA_3	GA_4	GA_{1+3+4}	IAA
Cell length	1	-0.932**	-0.899*	-0.536	-0.817*	0.410	0.461	0.791	0.822*	-0.725
Cellulose		1	0.967**	0.695	0.945**	-0.527	-0.612	-0.581	-0.625	0.550
Hemicelluloses			1	0.602	0.890*	-0.431	-0.474	-0.641	-0.675	0.493
Starch				1	0.848*	-0.927**	-0.332	-0.241	-0.292	-0.052
Sucrose					1	-0.755	-0.563	-0.466	-0.518	0.388
GA_1						1	0.144	0.257	0.302	0.052
GA_3							1	-0.155	-0.106	-0.487
GA_4								1	0.998**	-0.589
GA_{1+3+4}									1	-0.604
IAA										1

All the data were correlation coefficients. Significant differences were indicated at * P < 0.05 or ** P < 0.01.

GA_4 (Pearson correlation coefficient is 0.814, P < 0.05, Table S2), indicated GA_4 possibly regulated the expression of *XET2* in scape development. Besides, the sugars content was negatively correlated GA_1 and cell length, suggested sugars possibly playing roles in cell elongation (Table 1; Table S2). IAA level was positively correlated with the expression of *cyclin-SDS* (Pearson correlation coefficient is 0.980, P < 0.01, Table S2), demonstrated auxin regulating cell cycle rather than cell size in *Agapanthus* scape.

Discussion

GA and IAA Signals Regulated *Agapanthus* Scape Elongation

The use of plant growth regulators is an efficient way for plant height regulation (Wang et al. 2015). Numerous reports showed that PAC reduced plant height by inhibiting GAs biosynthesis, suggesting that bioactive GAs are critical for plant stem elongation (Zheng et al. 2012). Furthermore, GAs

perform their functions by crosstalk with other hormonal signals (Wang et al. 2015); for instance, GA and IAA targeted the activity of specific sets of transcripts that regulated cell proliferation and cell elongation (Gou et al. 2010; Lv et al. 2014). In this study, we reported that PAC reduced *Agapanthus* scape length by regulating bioactive GAs and IAA levels, and these hormones synergistically modulated cell proliferation and expansion. Furthermore, the morphological observation demonstrated that the cell length rather than the cell number decreased, indicating the dwarf traits mainly resulted from abnormal cell elongation. Correlation analysis indicated GA promoted cell expansion and IAA regulated cell proliferation in *Agapanthus* scape development.

GA Promoted Cell Elongation

GA was proved a key regulator of stem growth in plants (Wang et al. 2015). GAs were mainly synthesized in leaves, transported to shoot apex in floral initiation and transition via the phloem and vascular bundle (Hedden and Sponsel 2015). Our results showed GAs were likely transported from bottom to top via the vascular bundle in *A. praecox* ssp. *orientalis* scape, and PAC spray on leaves reduced bioactive GAs supply in scape elongation. Consequently, the regulatory network of GA signal was changed.

GA signal network provides a common mechanism for GAs homeostasis (Middleton et al. 2012; Davière and Achard 2016). In recent years, many genes in GA biosynthesis and signal transduction pathways have been identified (Sun 2011; Claeys et al. 2014). In the successive GA biosynthesis pathway, late steps of GA biosynthetic enzymes are particular response for bioactive GAs levels (Sun 2011). In this study, GAs biosynthesis was inhibited by PAC and the transcriptional level of *GA20ox*, which encodes an enzyme that catalyzes the late steps in the formation of bioactive GAs, was upregulated 6.06-16.21 (FC), suggesting feedback regulation of GA biosynthesis pathway. Likewise, GA signal-related genes also showed negative feedback mechanisms. Similar results were observed in *Daucus carota*, for the expression of *GA20ox1*, *GA20ox1*, *GID1b* and *GID1c* were upregulated with PAC treatment (Wang et al. 2015). In *Sorghum bicolor*, remarkable increase of five *DELLAs* expression were observed responding to exogenous PAC (Gao et al. 2012). Indeed, feedback regulation of GA biosynthesis in plants is firmly established as a mechanism to maintain GA homeostasis (Middleton et al. 2012).

GAs stimulate cell expansion that contributes to plant organ growth (Claeys et al. 2014). The plant cellular program is achieved by the enzymatic rearrangement of existing cell wall polymers and reorganization of their syntheses. GA stimulates cell expansion by inducing the expression of *XETs*, which play important roles in the restructuring of cell wall components that allow turgor-driven cell expansion (Jan et al. 2004; Claeys et al. 2014).

Many studies have proved sugars are involved in cell expansion (Kutschera and Niklas 2013). The process of scape elongation is coupled with increased substance metabolism, and sugar accumulation provides nutrients that are critical for this process. In plants, starch degraded into sucrose that can be utilized for vegetative growth. GA induces the activity of amylase that promotes starch degradation and PAC controls excessive vegetative growth by improving carbohydrate accumulation and GAs balance (Zheng et al. 2012). As a result, the accumulation of starch and sucrose provides a foundation for cell wall polysaccharide metabolism.

Cell Wall Modification Determined Cell Size

The plant cell wall determines the shape and size of cells. Plant cell walls are consist of cellulose fibrils tethered by hemicelluloses and embedded in pectins and glycoproteins (Carpita and Gibeaut 1993; Chen et al. 2013). Plant cell expansion requires the selective loosening and rearrangement of the cellulose/hemicelluloses network (Szymanski and Cosgrove 2009). *CESA* and *UXS* are responsible for the syntheses of cellulose and hemicelluloses, whereas *XET* cleaves xyloglucan hemicelluloses chains that crosslink cellulose microfibrils, contributing to cell wall loosening (Zhu et al. 2012). In this study, the transcriptional levels of *CESA* and *UXS* accorded with the contents of cellulose and hemicelluloses in dwarf scape suggested that polysaccharide accumulation possibly strengthened the stretch-resistant network of the cell wall, whereas cell wall loosening-related gene *XET2* was nearly silenced and cell wall loosening was repressed severely. Similar expression patterns were observed in *Populus* and *Brassica oleracea*, such that genes encoding *CESA* and *UXS* were upregulated in dwarf plants, while the expression of *XETs* were downregulated (Gou et al. 2010; Xie et al. 2014). In cotton (*Gossypium hirsutum*), both *XETs* and expansins are downregulated with mepiquat chloride (an inhibitor of GA biosynthesis), indicating GA positively regulate the expression of cell wall relaxation-related genes that promote cell elongation (Wang et al. 2014). These results implied that GA played pivotal roles in the network of cellular synthetic and metabolic pathways, and cell size was changed because of cell wall structure modification.

Auxin Regulated Cell Proliferation

Auxin is known to activate cell division-related genes that promote cell proliferation (Vanneste and Friml 2009). IAA is mobilized by directional transport to provide its precise distribution along a gradient in various organs and plays key

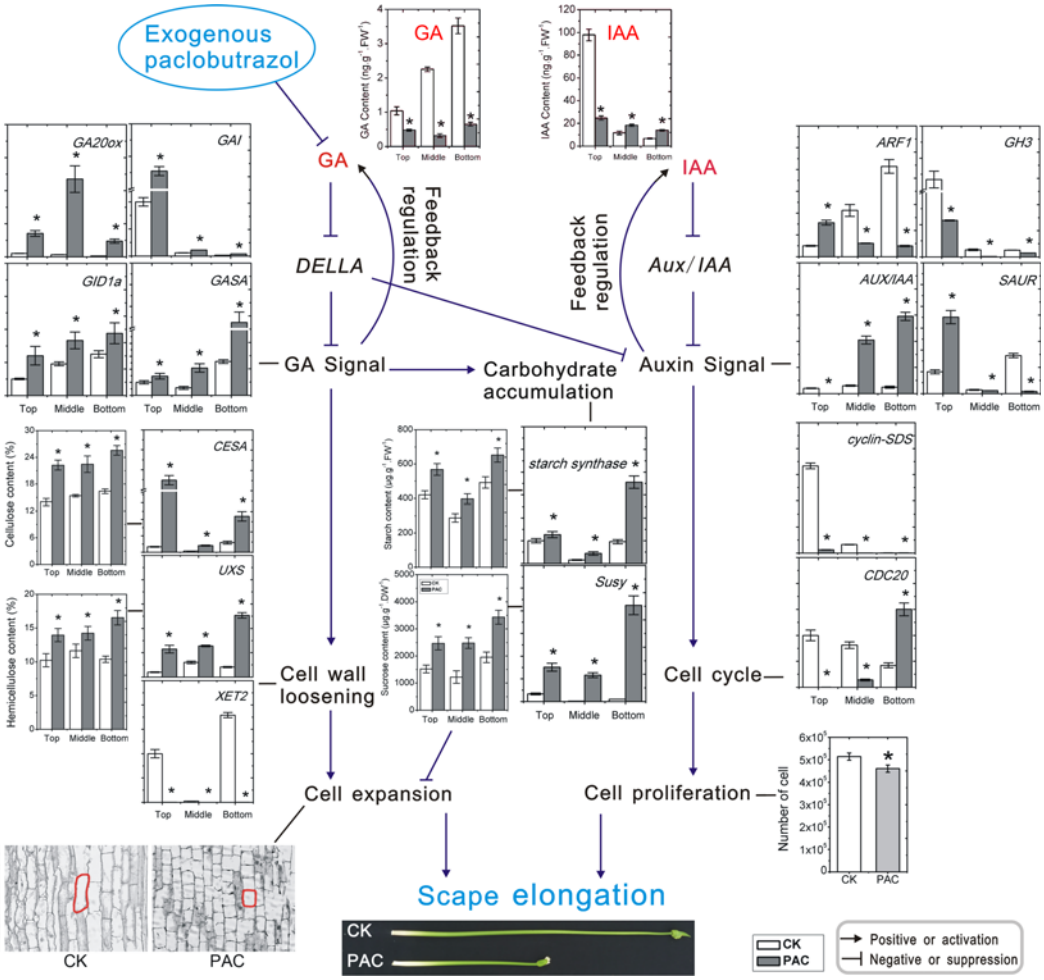

Fig. 6 Schematic representation of GA and IAA signals regulate the scape development in *A. praecox* ssp. *orientalis*.

roles in plant development. The expression of *Aux/IAA*, *ARF*, *SAUR*, and *GH3* triggers hormones signaling cascades, and auxin provides feedback regulation by regulating the expression and localization (Vanneste and Friml 2009). In this study, the expression patterns of *Aux/IAA*, *ARF*, *SAUR*, and *GH3* suggested PAC repressed auxin signaling (Fig. 3B). In *A. thaliana*, *SAUR36* was induced by PAC and depressed by GA_3, integrated auxin and GA signals to regulate hypocotyl elongation synergistically (Stamm and Kumar 2013). Cyclin-dependent kinases (*CDKs*) and cyclins regulate cell cycle progression (Bulankova et al. 2013). Cyclin proteins are accorded with cell proliferation since they show patterns of accumulation and destruction that are specific to different phases of the cell cycle in Arabidopsis (Donnelly et al. 1999). The meiosis specific *Cyclin-SDS* plays a specific role in regulating synapsis in prophase I of Arabidopsis (Guanfang et al. 2004), whereas *CDC20* play roles in the metaphase-anaphase transition in Arabidopsis (Kevei et al. 2011). These cell circle-related genes were accorded with IAA levels, suggesting auxin regulated cell circle that affected cell proliferation in scape elongation.

Conclusions

The application of PAC decreased endogenous bioactive GAs levels that induced dwarf scape in *A. praecox* ssp. *orientalis*. The inhibition of GA signaling triggered significant changes in auxin signaling and sugar metabolism that induced dwarf scape by inhibiting cell elongation and cell proliferation (Fig. 6). GA_4 and IAA levels positively correlated with the expression of *XET2* and *cyclin-SDS*, respectively, suggested that GA regulated cell expansion and IAA modulated cell proliferation. Integrated hormonal signal changes triggered downstream signaling cascades that induced final physiological responses during scape elongation in *A. praecox* ssp. *orientalis*. Our study provides basic data for the biological regulation mechanisms of dwarfism in this ornamental plant, which is helpful to improve scape morphogenesis via exogenous regulation and genetic approach in bulbous-flower.

Materials and Methods

Plant Materials and Growth Conditions

Four-year-old *A. praecox* ssp.*orientalis* were grown in the greenhouse of the experimental teaching center of Shanghai Jiao Tong University, Shanghai, China (31°01'31"N, 121°26'11"E), under natural light conditions with an indoor temperature of 20-25°C at night and 25-35°C during the day, a 16-h photoperiod, 60% relative humidity, and with photosynthetically active radiation of approximately 4000 μmol m^{-2} s^{-1}. The plants were planted in pots (30-cm diameter and 30-cm deep) filled with a mixture of vermiculite/peat (1:1, v/v) as a cultivation substrate. All the plants conducted by a routine management.

Application of PAC and Sample Collection

PAC (Sigma-Aldrich, St Louis, USA) was applied to regulate scape development of *A. praecox* ssp. *orientalis*. A 400 mg·L^{-1} solution of PAC was made with distilled water. Each of the control and PAC-treated plant leaves were sprayed with 20 mL distilled water and PAC solution, respectively. The treatment was performed every two weeks from January 20 until May 10. Both the control and PAC-treatment groups were conducted three replications, each group contained 8 plants. Scape length was examined every 5 days from May 10 until July 15. The scape samples from top, middle and bottom parts were collected respectively, when the floral bracts cracked.

Light Microscopy Observation

The fresh samples of control and PAC-treated were fixed immediately in formalin/acetic acid/70% ethanol (FAA, 5:5:90, v/v/v), dehydrated in an ethanol series, immersed with xylene, and embedded in paraffin. Sections were cut to a thickness of 8-10 μm. Slides were stained with safranin O (Sigma) to observe cell size and stained with periodic acid-Schiff (PAS) to identify polysaccharides. Microscopic observations were performed using a Leica DM2500 microscope (Leica Microsystems, Wetzlar, Germany). Cell longitudinal length was calculated by 10 individual cells of control and PAC-treated samples. Cell proliferation was investigated by using the data of scape length and single cell size. Cell number was calculated by the formula below: cell number = scape length/cell longitudinal length.

Quantification of Bioactive GAs and IAA

GAs and IAA quantification were conducted by the same method (Gou et al. 2010). Approximately 0.5 g fresh samples were frozen immediately in liquid N_2 and homogenized in 5 mL extraction mixture containing methanol/water/formic acid (15:4:1, v/v/v) and 20 mg·L^{-1} sodium diethyldithiocarbamate. The internal standards, including 25 ng $^2H_2$-GA_1, $^2H_2$-GA_3, $^2H_2$-GA_4 and 50 ng $^{13}C_6$-IAA (Sigma) were added to the extracts. The extracts were then centrifuged at 10,000 × *g* (Multifuge X1R; Thermo Fisher Scientific, Waltham, MA, USA) for 30 min after an overnight incubation at -20°C. The pooled supernates were passed through a Sep-Pak plus C^{18} cartridge, and the extractions were reduced to dryness *in vacuo* at 40°C, dissolved in 5 mL of 1 M formic acid, and passed through a MAX (mixed-mode cation exchange) column (Waters, Milford, MA, USA). The MAX column was washed with 5 mL of a solution containing 1 M formic acid, 0.1 M NH_4OH, and 0.1 M NH_4OH in 60% methanol. The samples were eluted with 5 mL 1.25 M formic acid in 70% methanol, and the eluates were evaporated *in vacuo*. The dry samples were redissolved in 50 μL formic acid/methanol (9:1, v/v) and passed through a 0.22-μm filter. Ten-microliter aliquots of the filtrates were analyzed by high-performance liquid chromatography-electrospray ionization ion trap tandem mass spectrometry (HPLC-ESI-Ion trap MS, Thermo Fisher). Mass spectrometry data were quantified by reference to the internal standards using M^+ ratios in equations for isotope dilution analysis, and total GAs was calculated by using the data of GA_1, GA_3 and GA_4. Each experiment was repeated three times.

GAs and IAA Immunolocalization

Scape tissues collected from top, middle and bottom were pre-fixed immediately in ethyl-3-(3-dimethylaminopropyl carbodiimide)/100 mM phosphate-buffered saline (PBS), and post-fixed in glutaraldehyde/paraformaldehyde/100 mM PBS (2.5:4:100, w/v/v). The fixed tissues were embedded in paraffin. Sections were cut to thickness of 8-10 μm and pasted onto poly-lysine slides. Tissue slides were deparaffinized, rehydrated, and rinsed in 10 mM PBS. Sections were immersed in blocking solution for 45 min. Thereafter, slides were washed in a regular salt rinse solution (RSR) and treated with 10 mM PBS/Triton X-100/BSA (99:0.8:0.1, v/v/w). Primary rat monoclonal antibody to GAs (catalog number: ab37243; Abcam, Cambridge, UK) and rabbit polyclonal antibody to IAA (catalog number: ab53359, Abcam) were diluted for 100 times, and tissue sections were incubated with the diluted antibodies in the dark at 37°C for 30 min. After rinsing in a high-salt rinse solution, tissue sections were incubated with anti-rat (catalog number: SA00002-6; Proteintech group, Inc., Chicago, IL, USA) secondary antibody (IgG alkaline phosphatase conjugates, Proteintech Group) and anti-rabbit (catalog number: SA00002-5) secondary antibody (IgG alkaline phosphatase conjugates, Proteintech Group) respectively, in the dark at 37°C for 30 min. After rinsing in RSR and PBS, microscopy was conducted to detect antibody signals. Microscopic observations were carried out using a Leica DM2500 microscope (Leica Microsystems, Wetzlar, Germany). To ensure the specificities of the antibody signals, negative controls were examined in which the primary antibody had been omitted and the sections were directly incubated with secondary antibodies, and blank controls were examined in which both the primary antibody and secondary antibody had been omitted.

Starch and Sucrose Quantification

Approximately 0.1 g frozen tissues were ground to a fine powder in 5 mL 80% (v/v) ethanol for starch assay. After centrifugation at 5,000 × *g* for 10 min, the pellet was washed with distilled water. The starch was extracted from the pellet in 5 mL 80% (w/v) calcium nitrate. A 200 μL solution of 5 mM I_2-KI was added to the starch solution and examined by ultraviolet spectrophotometer (Thermo) at 620 nm. Each experimentwas replicated three times.

For sucrose quantification, samples containing 0.2 g fresh tissues were homogenized in 2 mL 80% (v/v) ethanol and centrifuged for 5 min at 5,000 × *g*. The supernate was recovered and the pellets were re-extracted twice more. An aliquot (0.1 mL) of the concentrated solution was treated with 30% (w/v) potassium hydroxide (KOH) and incubated at 100°C for 10 min. Sucrose levels were quantified by the anthrone-sulfuric acid assay. The data were normalized to a sucrose standard curve, and each test was performed in triplicate.

Cellulose and Hemicelluloses Determination

The dried powdery samples were used for cell wall components digestion to extract cellulose and hemicelluloses (Peng, Hocart et al. 2000). We used potassium phosphate buffer (pH 7.0), chloroform/methanol (1:1, v/v), dimethyl sulfoxide/water (9:11, v/v) and 0.5% (w/v) ammonium oxalate to remove the components of soluble sugar, lipids, starch and pectin successively. Then the remaining pellet was extracted with 4 M KOH containing 1.0 mg·mL^{-1} sodium borohydride

for 1 h at room temperature. The combined supernatant with two parallel, one parallel was neutralized, dialyzed and lyophilized as KOH-extractable hemicelluloses monosaccharides. The other one parallel was collected to determine free pentoses. Then one of the remaining non-KOH-extractable residues was extracted with TFA for monosaccharides. The other one parallel was further extracted by 67% (v/v) sulfuric acid (H_2SO_4) for 1 h at 25°C and the supernatants were collected for determination of total cellulose and non-KOH-extractable hemicelluloses.

Ultraviolet spectrophotometer (Thermo) was used for collecting absorbance. Hexoses were detected using the anthrone-sulfuric acid method (Peng et al. 2000). Summarily, 1.0 mL aqueous samples containing 20-200 mg of hexoses was added to 2.0 mL 0.2% anthrone in concentrated H_2SO_4, and incubated with the boiling water bath for 5 min. After cooling, the absorbance was tested at 620 nm. Pentoses were detected using the orcinol-hydrochloric acid method. Briefly, 1.0 mL aqueous samples containing 20-200 mg of pentoses was added to 134.0 mL 6% orcinol/ethanol (v/v), and followed by 2.0 mL 0.1% ferric chloride in concentrated hydrochloric acid and incubated with the boiling water bath for 20 min. After cooling to 25°C, the sample absorbance was detected at 620 nm. The standard curves for hexoses and pentoses were plotted using D-glucose (Sigma) and D-xylose (Sigma) as standards, respectively. All experiments were carried out in biological triplicate.

Gene Expression Analysis

For gene expression analysis, frozen tissues from top, middle and bottom parts of scape described above were prepared. For each tissue, total RNA was extracted using the Trizol reagent (Invitrogen, Carlsbad, CA, USA) according to the manufacturer's instructions. RNA was purified using the DNase I and RNase inhibitors (TaKaRa, Kyoto, Japan). The cDNA was synthesized using the SYBR PrimeScript RT-PCR Kit II (TaKaRa), and first-strand cDNA prepared was used as a template. The relative expression levels of genes were measured using the SYBR Premix EX *Taq* II kit (Takara) according to the manufacturer's instructions. Real-time quantitative PCR (qRT-PCR) was performed on the Chromo4 Gradient Cycler system (Bio-Rad, Hercules, CA, USA). A gene encoding *Agapanthus β-actin* was used as the endogenous control. Triplicate quantitative PCR experiments were performed for each sample, and the expression values obtained were normalized against *β-actin*. All primer sequences are presented in Table S1. Analysis of the relative gene expression data was conducted using the $2^{-\Delta\Delta Ct}$ method (Livak and Schmittgen 2001).

Statistical Analysis

All data were presented as the mean values ± standard deviation (SD). The differences were statistically analyzed by one-way ANOVA and least significant difference (LSD) test ($P < 0.05$). Correlation analysis was used SPSS 19.0 software (IBM Corporation, Armonk, NY, USA).

Acknowledgements

The work received generous supports from the National Natural Science Foundation of China (NO. 31370695), Key Projects of the Shanghai Agricultural Committee (2010-6-2) and Shanghai Jiao Tong University 'Agri-X' Interdisciplinary Research Foundation (NO. 2015003). We thank Prof. Xiang-ning Jiang (Beijing Forestry University, China) for his excellent technical assistance in the quantitative analyses of GAs and IAA. The authors thank Dr. Wei-ming Wang for the linguistic modification.

Author's Contributions

XHS and DZ conceived and designed the experiments. JHY performed the experiments. JHY, DZ and LR analyzed the data. XHS contributed reagents/materials/analysis tools. JHY and DZ drafted the manuscript.

Supporting Information

Fig. S1. PAC-treating induced dwarf scape in *A. praecox* ssp. *orientalis.*
Table S1. Primers used for qRT-PCR.
Table S2. Correlation analysis of hormonal contents, sugars and related genes.

References

Ayano M, Kani T, Kojima M, Sakakibara H, Kitaoka T, Kuroha T, Angeles-Shim RB, Kitano H, Nagai K, Ashikari M (2014) Gibberellin biosynthesis and signal transduction is essential for internode elongation in deepwater rice. Plant Cell Environ 37:2313–2324

Bulankova P, Akimcheva S, Fellner N, Riha K (2013) Identification of *Arabidopsis* meiotic cyclins reveals functional diversification among plant cyclin genes. PLoS Genet 9:e1003508

Carpita NC, Gibeaut DM (1993) Structural models of primary cell walls in flowering plants: consistency of molecular structure with the physical properties of the walls during growth. Plant J 3:1–30

Chen IJ, Lo W, Chuang J, Cheuh C, Fan Y, Lin L, Wu S, Wang L (2013) A chemical genetics approach reveals a role of brassinolide and cellulose synthase in hypocotyl elongation of etiolated *Arabidopsis* seedlings. Plant Sci 209:46–57

Chen S, Gao R, Wang H, Wen M, Xiao J, Bian N, Zhang R, Hu W, Cheng S, Bie T, Wang X (2015) Characterization of a novel reduced height gene (*Rht23*) regulating panicle morphology and plant architecture in bread wheat. Euphytica 203:583–594

Christiaens A, Pauwels E, Gobin B, Van Labeke MC (2015) Flower differentiation of azalea depends on genotype and not on the use of plant growth regulators. Plant Growth Regul 75:245–252

Claeys H, De Bodt S, Inzé D (2014) Gibberellins and DELLAs: central nodes in growth regulatory networks. Trends Plant Sci 19:231–239

Cosgrove DJ (2005) Growth of the plant cell wall. Nat Rev Mol Cell Biol 6:850–861

Dai Y, Wang H, Li B, Huang J, Liu X, Zhou Y, Mou Z, Li J (2006) Increased expression of MAP KINASE KINASE7 causes deficiency in polar auxin transport and leads to plant architectural abnormality in *Arabidopsis*. Plant Cell 18:308–320

Davière J, Achard P (2016) A pivotal role of DELLAs in regulating multiple hormone signals. Mol Plant 9:10–20

Dayan J, Voronin N, Gong F, Sun T, Hedden P, Fromm H, Aloni R (2012) Leaf-induced gibberellin signaling is essential for internode elongation, cambial activity, and fiber differentiation in tobacco stems. Plant Cell 24:66–79

Donnelly PM, Bonetta D, Tsukaya H, Dengler RE, Dengler NG (1999) Cell cycling and cell enlargement in developing leaves of *Arabidopsis*. Dev Biol 215:407–419

Feng S, Martinez C, Gusmaroli G, Wang Y, Zhou J, Wang F, Chen L, Yu L, Iglesias-Pedraz JM, Kircher S, Schäfer E, Fu X, Fan L-M, Deng XW (2008) Coordinated regulation of *Arabidopsis thaliana* development by light and gibberellins. Nature 451:475–479

Gao S, Xie X, Yang S, Chen Z, Wang X (2012) The changes of GA

level and signaling are involved in the regulation of mesocotyl elongation during blue light mediated de-etiolation in *Sorghum bicolor*. Mol Biol Rep 39:4091–4100

Gou J, Strauss SH, Tsai CJ, Fang K, Chen Y, Jiang X, Busov VB (2010) Gibberellins regulate lateral root formation in *Populus* through interactions with auxin and other hormones. Plant Cell 22:623–639

Guanfang W, Hongzhi K, Yujin S, Zhang X, Zhang W, Altman N, dePamphilis CW, Ma H (2004) Genome-wide analysis of the cyclin family in *Arabidopsis* and comparative phylogenetic analysis of plant cyclin-like proteins. Plant Physiol 135:1084–1099

Hedden P, Sponsel V (2015) A century of gibberellin research. J Plant Growth Regul 34:740–760

Hepworth J, Lenhard M (2014) Regulation of plant lateral-organ growth by modulating cell number and size. Curr Opin Plant Biol 17:36–42

Jan A, Yang G, Nakamura H, Ichikawa H, Kitano H, Matsuoka M, Matsumoto H, Komatsu S (2004) Characterization of a xyloglucan endotransglucosylase gene that is up-regulated by gibberellin in rice. Plant Physiol 136:3670–3681

Kevei Z, Baloban M, Da Ines O, Tiricz H, Kroll A, Regulski K, Mergaert P, Kondorosi E (2011) Conserved *CDC20* cell cycle functions are carried out by two of the five isoforms in *Arabidopsis thaliana*. PLoS One 6:e20618

Kutschera U, Niklas KJ (2013) Cell division and turgor-driven stem elongation in juvenile plants: a synthesis. Plant Sci 207:45–56

Livak KJ, Schmittgen TD (2001) Analysis of relative gene expression data using real-time quantitative PCR and the $2^{-\Delta\Delta CT}$ method. Methods 25:402–408

Lv H, Zheng J, Wang T, Fu J, Huai J, Min H, Zhang X, Tian B, Shi Y, Wang G (2014) The maize *d2003*, a novel allele of VP8, is required for maize internode elongation. Plant Mol Biol 84:243–257

Mashiguchi K, Tanaka K, Sakai T, Sugawara S, Kawaide H, Natsume M, Hanada A, Yaeno T, Shirasu K, Yao H, McSteen P, Zhao Y, Hayashi K, Kamiya Y, Kasahara H (2011) The main auxin biosynthesis pathway in *Arabidopsis*. Proc Natl Acad Sci USA 108:18512–18517

Middleton AM, Úbeda-Tomás S, Griffiths J, Holman T, Hedden P, Thomas SG, Phillips AL, Holdsworth MJ, Bennett MJ, King JR (2012) Mathematical modeling elucidates the role of transcriptional feedback in gibberellin signaling. Proc Natl Acad Sci USA 109:7571–7576

Nemhauser JL, Hong F, Chory J (2006) Different plant hormones regulate similar processes through largely nonoverlapping transcriptional responses. Cell 126:467–475

Peng L, Hocart CH, Redmond JW, Williamson RE (2000) Fractionation of carbohydrates in *Arabidopsis* root cell walls shows that three radial swelling loci are specifically involved in cellulose production. Planta 211:406–414

Serrani J, Fos M, Atarés A, GarcíaMartínez J (2007) Effect of gibberellin and auxin on parthenocarpic fruit growth induction in the cv Micro-Tom of tomato. J Plant Growth Regul 26:211–221

Stamm P, Kumar P (2013) Auxin and gibberellin responsive *Arabidopsis* SMALL AUXIN UP RNA36 regulates hypocotyl elongation in the light. Plant Cell Rep 32:759–769

Sun T (2011) The molecular mechanism and evolution of the GA–GID1–DELLA signaling module in plants. Curr Biol 21:338–345

Szymanski DB, Cosgrove DJ (2009) Dynamic coordination of cytoskeletal and cell wall systems during plant cell morphogenesis. Curr Biol 19:800–811

Takatsuka H, Ohno R, Umeda M (2009) The *Arabidopsis* cyclin-dependent kinase-activating kinase *CDKF;1* is a major regulator of cell proliferation and cell expansion but is dispensable for *CDKA* activation. Plant J 59:475–487

Topp SH, Rasmussen SK (2012) Evaluating the potential of *SHI* expression as a compacting tool for ornamental plants. Plant Sci 187:19–30

Vanneste S, Friml J (2009) Auxin: a trigger for change in plant development. Cell 136:1005–1016

Vivian-Smith A, Koltunow AM (1999) Genetic analysis of growth-regulator-induced parthenocarpy in *Arabidopsis*. Plant Physiol 121:437–452

Wang G, Que F, Xu Z, Wang F, Xiong A (2015) Exogenous gibberellin altered morphology, anatomic and transcriptional regulatory networks of hormones in carrot root and shoot. BMC Plant Biol 15:1–12

Wang L, Mu C, Du M, Chen Y, Tian X, Zhang M, Li Z (2014) The effect of mepiquat chloride on elongation of cotton (*Gossypium hirsutum* L.) internode is associated with low concentration of gibberellic acid. Plant Sci 225:15–23

Xie Q, Chen G, Chen X, Deng L, Liu Q, Zhang Y, Hu Z (2014) Jointly silencing *BoDWARF*, *BoGA20ox* and *BoSP* (*SELF-PRUNING*) produces a novel miniature ornamental *Brassica oleracea* var. *acephala* f. tricolor variety. Mol Breeding 34:99–113

Yamaguchi S (2008) Gibberellin metabolism and its regulation. Annu Rev Plant Biol 59:225–251

Zhang D, Ren L, Yue J, Wang L, Zhuo L, Shen X (2013) A comprehensive analysis of flowering transition in *Agapanthus praecox* ssp. *orientalis* (Leighton) Leighton by using transcriptomic and proteomic techniques. J Proteomics 80:1–25

Zhang D, Ren L, Yue J, Wang L, Zhuo L, Shen X (2014) GA_4 and IAA were involved in the morphogenesis and development of flowers in *Agapanthus praecox* ssp. *orientalis*. J Plant Physiol 171:966–976

Zheng R, Wu Y, Xia Y (2012) Chlorocholine chloride and paclobutrazol treatments promote carbohydrate accumulation in bulbs of *Lilium* Oriental hybrids 'Sorbonne'. J Zhejiang Univ Sci B 13:136–144

Zhu X, Shi Y, Lei G, Fry SC, Zhang B, Zhou Y, Braam J, Jiang T, Xu X, Mao C, Pan Y, Yang J, Wu P, Zheng S (2012) *XTH31*, encoding an in vitro XEH/XET-active enzyme, regulates aluminum sensitivity by modulating in vivo XET action, cell wall xyloglucan content, and aluminum binding capacity in *Arabidopsis*. Plant Cell 24:4731–4747